The Eye as a Window to the Brain: Neuroretinal Thickness Is Associated With Microstructural White Matter Injury in HIV-Infected Children

Charlotte Blokhuis,[1] Nazli Demirkaya,[2] Sophie Cohen,[1] Ferdinand W. N. M. Wit,[3–5] Henriëtte J. Scherpbier,[1] Peter Reiss,[3–5] Michael D. Abramoff,[6,7] Matthan W. A. Caan,[8] Charles B. L. M. Majoie,[8] Frank D. Verbraak,[2,9,10] and Dasja Pajkrt[1]

[1]Department of Hematology, Immunology and Infectious Diseases, Emma Children's Hospital/Academic Medical Center, University of Amsterdam, The Netherlands
[2]Department of Ophthalmology, Academic Medical Center, University of Amsterdam, The Netherlands
[3]Department of Global Health, Academic Medical Center, University of Amsterdam, and Amsterdam Institute for Global Health and Development, The Netherlands
[4]Department of Internal Medicine, Division of Infectious Diseases, Center for Infection and Immunity Amsterdam (CINIMA), Academic Medical Center, Amsterdam, The Netherlands
[5]HIV Monitoring Foundation, Amsterdam, The Netherlands
[6]Department of Ophthalmology and Visual Sciences, Stephen A. Wynn Institute for Vision Research, University of Iowa, Iowa City, Iowa, United States
[7]Department of Biomedical Engineering and Department of Electrical and Computer Engineering, University of Iowa, Iowa City, Iowa, United States
[8]Department of Radiology, Academic Medical Center, University of Amsterdam, The Netherlands
[9]Department of Biomedical Engineering and Physics, Academic Medical Center, University of Amsterdam, The Netherlands
[10]Department of Ophthalmology, VU University Medical Center, Amsterdam, The Netherlands

Correspondence: Charlotte Blokhuis, Department of Pediatric Hematology, Immunology, and Infectious Diseases, Emma Children's Hospital/Academic Medical Center, Meibergdreef 9, 1105AZ Amsterdam, The Netherlands; c.blokhuis@amc.nl.

CB and ND contributed equally to the work presented here and should therefore be regarded as equivalent authors.

Submitted: April 8, 2016
Accepted: June 13, 2016

Citation: Blokhuis C, Demirkaya N, Cohen S, et al. The eye as a window to the brain: neuroretinal thickness is associated with microstructural white matter injury in HIV-infected children. *Invest Ophthalmol Vis Sci.* 2016;57:3864–3871. DOI:10.1167/iovs.16-19716

Purpose. Despite combination antiretroviral therapy (cART), perinatal HIV-infection can cause decreased gray and white matter volume, microstructural white matter injury, and retinal structural abnormalities. As neuroretinal tissue is directly connected to the brain, these deficits may have a shared pathogenesis. We aimed to assess associations between neuroretinal thickness and cerebral injury in cART-treated perinatally HIV-infected children and healthy controls.

Methods. This cross-sectional observational study included 29 cART-treated perinatally HIV-infected children and 35 matched healthy controls. All participants underwent 3.0 Tesla magnetic resonance imaging (MRI), determining gray and white matter volumes from T1-weighted sequences, and white matter diffusivity using diffusion tensor imaging (DTI). Regional individual and total neuroretinal layer thickness was quantified using spectral-domain optical coherence tomography. We explored associations between retinal and cerebral parameters using multivariable linear regression analysis.

Results. In HIV-infected children, lower foveal and pericentral neuroretinal thickness was associated with damaged white matter microstructure, in terms of lower fractional anisotropy and higher mean and radial diffusivity. In healthy controls only, neuroretinal thickness was associated with gray and white matter volume.

Conclusions. Decreased neuroretinal thickness is associated with microstructural white matter injury, but not with lower cerebral volume in HIV-infected children. This suggests that HIV-induced retinal thinning and microstructural white matter injury may share a common pathogenesis, and longitudinal assessment of neuroretinal alterations in parallel with MRI and neuroinflammatory markers may further our insight into the pathogenesis of HIV-induced cerebral injury in children.

Keywords: perinatally HIV-infected children, cerebral injury, magnetic resonance imaging, diffusion tensor imaging, retina, optical coherence tomography

The prevalence of severe central nervous system (CNS) abnormalities in HIV-infected children, such as HIV-encephalopathy, has decreased drastically since combination antiretroviral therapy (cART).[1] Nevertheless, cART treated HIV-infected children still encounter neurological and cognitive problems with macro- and microstructural cerebral damage that can occur subclinically.[2,3] Recently, we demonstrated lower brain volumes, increased white matter (WM) hyperintensities, and increased WM diffusivity in perinatally HIV-infected children on cART, as compared to matched healthy controls.[4]

The observed cerebral injury was associated with poorer cognitive performance in multiple neurocognitive domains.[4,5] Retinal thickness (RT) analysis using spectral-domain optical coherence tomography (SD-OCT) revealed a decrease in foveal thickness in the HIV-infected children compared to controls.[6] As the retina shares developmental, physiological, and anatomical features with the brain,[7] these retinal and cerebral deficits may have a shared pathogenesis, which could include HIV-induced impeded maturation or persistent neuroinflammation and neurodegeneration. The associations between a higher peak HIV viral load and both retinal and cerebral injury support this theory.[4,6]

Here, we examined associations of RT with cerebral volume and WM microstructural alterations in HIV-infected children and matched controls, using SD-OCT and advanced magnetic resonance imaging (MRI) techniques, including diffusion tensor imaging (DTI). Further, we evaluated whether the relationship between retinal and cerebral structure is affected by pediatric HIV infection.

As OCT has been successfully used to link retinal and intracerebral pathology in other neuroinflammatory and neurodegenerative diseases,[7–11] evaluating neuroretinal structure may increase our understanding of the pathogenesis of pediatric HIV-induced cerebral injury.

Methods

This study is part of an interdisciplinary observational cross-sectional case-control study, evaluating neurological and neurocognitive disorders, neuroradiological and ophthalmic alterations in perinatally HIV-infected children as compared to age, sex, ethnicity, and socio-economic status (SES) matched healthy controls in The Netherlands (NOVICE study, Dutch Trial Registry ID NTR4074).[4–6] The study adhered to the tenets of the Declaration of Helsinki and was approved by the investigational review board of the Academic Medical Center (AMC) in Amsterdam, The Netherlands. Written informed consent was obtained from all parents and from children aged 12 years and above.

Study Participants

The NOVICE study participants consisted of perinatally HIV-infected children aged 8 to 18 years, recruited from the AMC outpatient clinic, Amsterdam, and healthy controls, matched for age, sex, ethnicity, and SES as described previously.[5] Exclusion criteria for study participation were chronic HIV-unrelated neurological disease, (history of) intracerebral neoplasms, traumatic brain injury, psychiatric disorders, and MRI contraindications. Additional ophthalmic exclusion criteria were high refractive errors (spherical equivalent [SE] exceeding +5.5 or −8.5 D), visual acuity below 0.1 on the logMAR chart, intraocular pressure higher than 21 mm Hg, significant media opacities, and a history of ocular surgery or ocular disease.

SD-OCT and Retinal Layer Segmentation

Spectral-domain optical coherence tomography images were obtained with the Topcon 3D OCT-1000 (Topcon, Inc., Paramus, NJ, USA) using the 3D macular and disc volume scan protocols. Only high-quality images with a Topcon image quality factor (QF) > 60 were used. From each 3D macular volume, individual neuroretinal layers were segmented automatically using the validated Iowa Reference Algorithms, allowing for all individual retinal layers thickness calculations for each of the nine macular regions as defined by the Early Treatment of Diabetic Retinopathy Study (ETDRS; as shown in Supplementary Fig. S1).[12,13] We selected foveal, pericentral, and peripheral ETDRS rings, as in previous studies.[6,14,15] Peripapillary retinal nerve fiber layer (RNFL) thickness measurements were acquired from the 3D optic nerve head OCTs using the same Iowa Reference Algorithms.[12,13] The peripapillary ring was centered manually if needed, with the center of the ring coinciding with the center of the optic disc.

MRI Data Acquisition and Data Processing

Brain scans were obtained using a 3.0 Tesla MRI scanner (Intera, Philips Healthcare, Best, The Netherlands) as previously described in further detail.[4] A nonlinear least squares estimation of diffusion tensors was used to compute fractional anisotropy (FA), mean diffusivity (MD), axial diffusivity (AD), and radial diffusivity (RD) maps, which were averaged over the entire skeleton to obtain whole brain WM DTI measures. T1-weighted images were automatically segmented (Freesurfer Image Analysis Suite v5.0.17, Charlestown, MA, USA) and manually checked for inaccuracies. White matter hyperintensity (WMH) prevalence and volume were derived from Fluid-Attenuated Inversion Recovery images using a semi-automated technique.

Statistical Analysis

Statistical analyses were performed using Stata Statistical Software, release 13 (StataCorp LP, College Station, TX, USA). Demographic/clinical characteristics were compared between the two groups using the Mann-Whitney U test or the χ^2 test, as appropriate. Group differences in RT were assessed by age-, sex-, and SE-adjusted mixed linear models, taking into account within-subject intereye correlations.[6] Group differences in MRI parameters were assessed using linear regression, adjusted for age and sex, and additionally for intracranial volume (ICV) in case of volumetric measurements.

Multivariable linear regression was used to assess associations between OCT (independent) and MRI (dependent) parameters, focusing on the macular regions and layers that differed between the two groups, as shown previously (foveal and pericentral total retina, inner retinal layers, and outer nuclear layer + inner segments [ONL + IS]).[6] Additionally, we explored the peripapillary RNFL, as RT in this area has previously been associated with MRI abnormalities in patients with dementia and multiple sclerosis.[16–18] Prior to analysis, RT values obtained from both eyes were averaged, and DTI values were multiplied by 100 to obtain easier-to-read coefficients. All analyses were corrected for age, sex, and SE, and additionally for ICV in case of volumetric outcomes. Correction for OCT scan QF was not applied, as mean QF was high and did not differ significantly between groups (median QF: HIV-infected = 85.78; controls = 86.37; $P = 0.710$). Considering the relatively small sample size, we performed only pooled analyses with HIV status as a covariable to generate more statistical power as compared to stratifying by HIV status.

We used a two-step analysis approach to evaluate the relationship between OCT and MRI parameters in our cohort. We first evaluated the associations between OCT and MRI parameters separately for HIV-infected and healthy participants, by stratifying only RT between the two groups and adding the two resulting variables (RT of HIV-infected participants and RT of healthy controls) to the basic model described above. In a separate analysis, we assessed whether being HIV-infected exerted a significant influence on the potential association between RT and cerebral injury (i.e., if the predictive value of RT on cerebral injury differed between

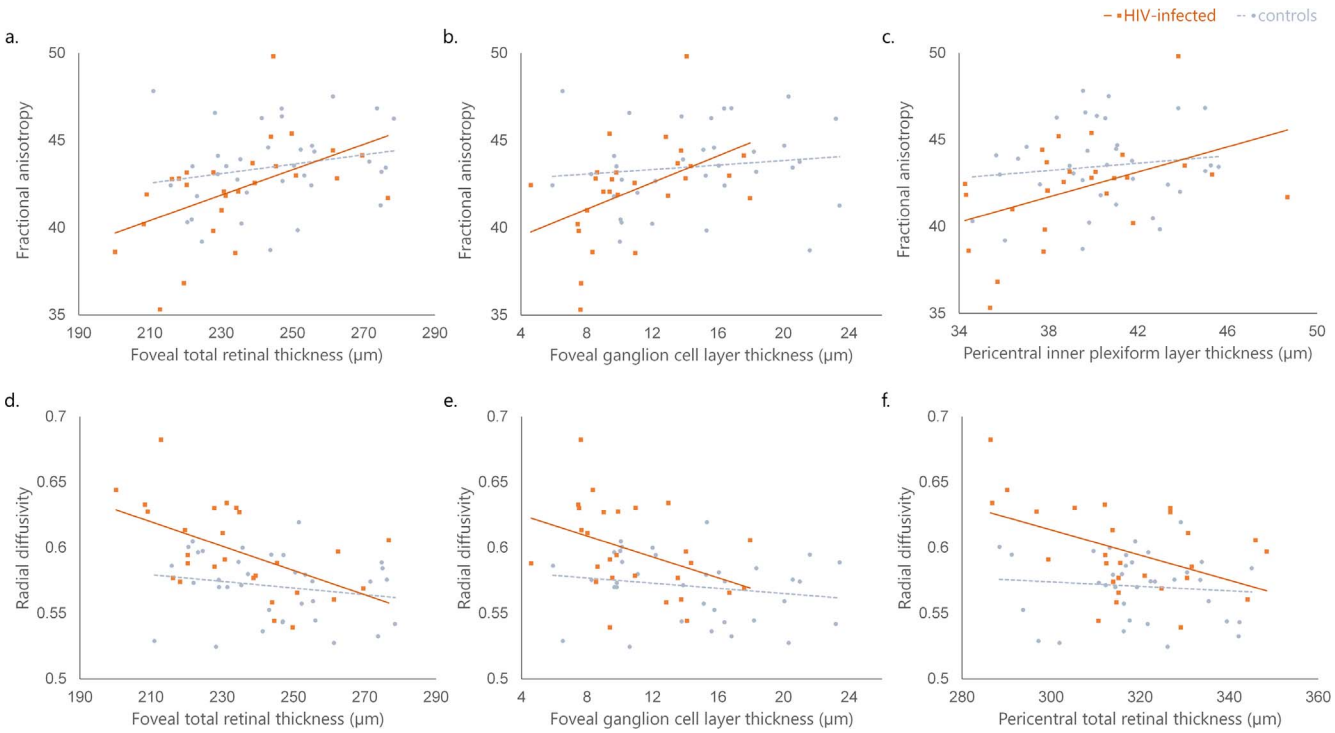

Figure 1. Associations between RT and WM microstructure in HIV-infected children and healthy controls. Univariable scatter and linear fit plots illustrating the associations between RT and FA (**a**, **b**, **c**) and RD (**d**, **e**, **f**) in HIV-infected children (*solid line*), which were absent in healthy controls (*dashed line*). Furthermore, the associations between RT in pericentral regions (**c**, **f**) and WM diffusivity were significantly different between the two participant groups (i.e., the interaction between HIV status and pericentral RT was significantly associated with WM diffusivity outcomes).

groups), by including RT and a HIV–RT interaction term in the basic model.

In line with the exploratory nature of this study, adjustment for multiple comparisons was not performed and statistical significance was set at a two-sided $P < 0.05$.

Results

Participant Characteristics

The NOVICE cohort consisted of 35 HIV-infected children and 37 healthy controls. Four HIV-infected children did not undergo MRI examination due to dental braces ($n = 2$), claustrophobia ($n = 1$), or lack of consent for the scan ($n = 1$). Two patients (one with a history of cytomegalovirus retinitis in both eyes; one who did not consent to OCT examination) and two controls (one with refractive error > +5.5D; one with fixation problems) were excluded from OCT. In addition, two left eyes of two HIV-infected children were excluded from analysis due to the presence of uveitis and congenital toxoplasmosis lesions, respectively.

Consequently, 29 HIV-infected children (median age, 13.1; interquartile range [IQR], 11.5–15.8) and 35 healthy controls (median age, 12.1; IQR, 11.5–15.7) were analyzed. Demographical data, clinical characteristics, and relevant OCT and MRI findings are displayed in Table 1. Age, sex, ethnicity, and parental employment did not differ significantly between groups. In the HIV-infected group, parental education level was slightly lower and more children were immigrants. Among HIV-infected children, 25 (86%) were on cART at time of study assessment, all of whom had undetectable plasma HIV viral loads. Median $CD4^+$ T-cell count was 800 cells/μL at time of assessment. With OCT, a significantly lower total foveal RT was detected in HIV-infected children, most prominently due to a thinner ONL + IS (median ONL + IS thickness: HIV-infected = 107.0 μm; controls = 111.8 μm; $P = 0.02$). On MRI scans, HIV-infected participants had a significantly lower total gray matter (GM) volume, as well as poorer WM integrity, as indicated by higher MD, RD, and AD, and lower FA.

RT and WM Diffusivity

Associations between OCT and DTI parameters in HIV-infected and healthy children are described in Table 2 (and displayed in further detail in Supplementary Tables S1, S2). Multiple correlations were found between RT and DTI parameters in HIV-infected children. A thinner RT (total retina as well as individual layers) was associated with higher MD and RD, and lower FA (Fig. 1); these findings were more pronounced in the foveal region. No significant correlations were observed between RT and AD in HIV-infected children. In healthy children, a thinner RT (foveal ONL + IS and pericentral total RT) was associated with lower AD (Supplementary Table S1). No significant associations were detected between peripapillary RNFL thickness and any DTI parameters for both HIV-positive children and controls.

The association between RT and WM diffusivity was significantly different between HIV-infected and healthy children, as indicated by HIV–RT interaction terms with $P < 0.05$ for several pericentral layers (total RT, ganglion cell layer [GCL], and inner plexiform layer [IPL] with MD, GCL with RD, and total RT with AD, as shown in Supplementary Table S2), but not for foveal layers.

RT and Cerebral Volumes

Results of the regression analysis of RT and cerebral volume measurements are summarized in Table 3 (and displayed in

Table 1. Participant Characteristics

	n	HIV-Infected, *n* = 29	Healthy Controls, *n* = 35	*P* Value
Demographic characteristics				
Male sex	–	16 (55)	16 (45)	0.567
Age at OCT, y	–	13.1 (11.5–15.8)	12.1 (11.5–15.7)	0.377
Ethnicity, black	–	22 (76)	24 (69)	0.238
Immigrant				
Child	–	19 (66)	2 (6)	<0.001*
1 or both parents	–	10 (34)	31 (88)	
SES				
Parental employment	–	1 (0–1)	1 (0–1)	0.449
Parental education (ISCED)	–	5 (4–6)	5 (5–6)	0.030*
HIV characteristics				
Age at HIV diagnosis, y	29	1.2 (0.6–4.2)	–	–
CDC stage, *n*				
N/A	29	9 (31)	–	–
B		12 (41)	–	–
C		8 (28)	–	–
HIV encephalopathy, *n*	29	2 (7)	–	–
Nadir $CD4^+$ T-cell *Z*-score	27	−0.7 (−1.5 to −0.4)	–	–
Peak viral load, log copies/mL	26	5.5 (5.1–5.9)	–	–
$CD4^+$ T-cell count at study inclusion, $*10^6$/L	28	800 (590–980)	–	–
Undetectable viral load, *n*	29	25 (86)	–	–
Current cART use, *n*	29	25 (86)	–	–
Duration of cART use, y	26	11.3 (7.1–14.7)	–	–
Optical coherence tomography				
Macula				
Foveal RT	–	232.1 (218.1–245.7)	245.2 (228.4–256.3)	0.020*
Pericentral RT	–	315.2 (310.1–327.2)	319.2 (312.6–328.3)	0.171
Peripheral RT	–	288.2 (270.5–295.6)	286.0 (274.7–292.1)	0.688
Peripapillary RNFL thickness	–	107.4 (99.4–122.1)	111.7 (101.8–118.2)	0.760
Magnetic resonance imaging				
T1-weighted				
Suitable for assessment	–	26 (89)	35 (100)	0.051
Total GM volume, cm^3	–	656 (640–708)	706 (627–755)	0.029*
Total WM volume, cm^3	–	436 (400–442)	439 (424–480)	0.168
FLAIR				
Suitable for assessment	–	25 (86)	33 (94)	0.270
WMH prevalence	–	16 (64)	6 (18)	<0.001*
WMH volume,† cm^3	–	52.3 (0–124.5)	0 (0–0)	<0.001*
DTI				
Suitable for assessment	–	27 (93)	35 (100)	0.114
FA	–	0.43 (0.41–0.44)	0.44 (0.42–0.47)	0.026*
MD, $*10^3$	–	0.79 (0.77–0.82)	0.77 (0.76–0.79)	<0.001*
RD, $*10^3$	–	0.59 (0.57–0.63)	0.57 (0.54–0.59)	<0.001*
AD, $*10^3$	–	1.19 (1.17–1.21)	1.17 (1.16–1.18)	<0.001*

All data are presented as median (IQR) or *n* (%). Nonblack ethnicity includes Creole, Hispanic, Caucasian, and mixed (i.e., Black/Caucasian, Asian/Caucasian). Group differences in demographical data were assessed using χ^2 or Fisher's exact tests for categorical data and the Mann-Whitney *U* test for continuous data. Group differences in RT were assessed using linear regression with mixed effects, adjusted for age, sex, and SE. Group differences in neuroimaging outcomes were assessed as follows: volumetric measurements using linear regression adjusted for age and sex, and ICV; WMH prevalence using logistic regression adjusted for age and sex; and DTI using linear regression adjusted for age and sex. ISCED, International Standard Classification of Education; CDC, Centers for Disease Control and Prevention; FLAIR, fluid-attenuated inversion recovery.

* $P < 0.05$.

† Median and IQR for all participants in each group.

detail in Supplementary Tables S3, S4). In healthy children, positive associations were found between thickness of several foveal and pericentral retinal layers and GM volume (Fig. 2). Furthermore, foveal GCL thickness was positively correlated with WM volume. However, we found no significant associations between peripapillary RNFL and cerebral volume in either group (Supplementary Table S3) or between RT and cerebral volume in the HIV-infected group. The HIV–RT interaction term was not significant for any of the detected associations between RT and cerebral volume (Supplementary Table S4).

Retinal thickness was not associated with WMH volume, although we detected a borderline significant association between thickness of the pericentral ONL + IS and WMH volume ($P = 0.051$).

Table 2. Associations Between RT and WM Diffusivity

	Fractional Anisotropy		Mean Diffusivity		Radial Diffusivity	
	Coefficient	*P* Value	Coefficient	*P* Value	Coefficient	*P* Value
Foveal layers						
Total RT						
HIV-infected	0.062	0.010*	−0.057	0.004*	−0.079	0.002*
Healthy	0.039	0.073	−0.018	0.310	−0.036	0.109
GCL						
HIV-infected	0.338	0.012*	−0.211	0.059	−0.344	0.016*
Healthy	0.127	0.152	−0.105	0.154	−0.155	0.101
IPL						
HIV-infected	0.299	0.014*	−0.186	0.063	−0.304	0.018*
Healthy	0.131	0.177	−0.105	0.196	−0.156	0.131
INL						
HIV-infected	0.431	0.000*	−0.253	0.012*	−0.427	0.001*
Healthy	0.171	0.087	−0.130	0.133	−0.198	0.065
ONL+IS						
HIV-infected	0.069	0.073	−0.057	0.075	−0.085	0.040*
Healthy	0.069	0.131	0.012	0.758	−0.030	0.533
Pericentral layers						
Total RT						
HIV-infected	0.047	0.110	−0.066	0.005*	−0.080	0.010*
Healthy	0.033	0.276	0.019	0.404	−0.004	0.908
GCL						
HIV-infected	0.195	0.029*	−0.200	0.005*	−0.275	0.003*
Healthy	0.061	0.485	0.073	0.293	0.020	0.825
IPL						
HIV-infected	0.360	0.008*	−0.259	0.020*	−0.400	0.005*
Healthy	0.094	0.499	0.066	0.564	−0.004	0.976
INL						
HIV-infected	0.156	0.186	−0.140	0.141	−0.199	0.111
Healthy	0.033	0.829	0.143	0.249	0.091	0.573
ONL+IS						
HIV-infected	−0.019	0.725	−0.024	0.594	−0.014	0.809
Healthy	0.044	0.416	0.032	0.462	0.002	0.979

Results of the pooled regression analysis evaluating the relationship between retinal layer thickness and WM diffusivity. The regression model included retinal layer thickness, which was stratified between HIV-infected children and controls (as displayed in the table), and covariables HIV status, age, sex, and SE (not shown). Coefficients represent the change in WM diffusivity outcomes ($\times 10^2$) per micron increase in RT. INL, inner nuclear layer.

* $P < 0.05$.

Discussion

In the current study, we assessed associations between RT and WM integrity and cerebral volume in perinatally HIV-infected children stable on cART, as compared to a group-wise matched healthy control group. Our findings indicate that RT is strongly associated with WM microstructure in HIV-infected children, and correlates with cerebral volume in healthy children. To our knowledge, this is the first study exploring RT as a potential tool to help elucidate the pathogenesis of cerebral injury in HIV, which hampers comparison of our findings to other studies.

HIV-infected children had a significantly lower FA, higher RD, and higher MD compared to the healthy group, all indicative of reduced WM integrity.[4] In a previous report comparing these same two groups, we described a significant decrease in foveal RT (and to a lesser degree pericentral RT) in the HIV-infected group, mostly caused by thinner neuroretinal layers and ONL + IS.[6] In the current study, the thickness of these retinal layers proved to be strongly associated with DTI outcomes in the HIV-infected group. The directions of associations between RT and WM diffusivity were shown to be consistent with our hypothesis that retinal structural alterations occur in parallel with cerebral injury, as reflected by lower FA, higher MD, and higher RD.[4]

Our results are suggestive of a shared pathogenesis of observed WM microstructural alterations and retinal thinning, which could include HIV-induced impeded maturation of the retina and WM, and/or persistent neuroinflammation and neurodegeneration.[2] Interestingly, a significant influence of HIV on the relationship between RT and WM diffusivity was only apparent in the pericentral retinal region, but not in the foveal region (as shown in Supplementary Table S2). Foveal RT and WM diffusivity were both affected in HIV-infected children. Conversely, pericentral RT did not differ between cases and controls. Despite this, associations between pericentral RT and WM diffusivity were found exclusively in HIV-infected children, who had higher WM diffusivity as compared to controls. This results in a different predictive value of pericentral RT for WM diffusivity in HIV-infected children, as reflected by the significant HIV–RT interaction term. These findings may imply that pericentral RT is affected by HIV infection via similar mechanisms that underlie foveal and WM

Table 3. Associations Between Retinal Thickness and Cerebral Volumes

	GM Volume		WM Volume		WMH Volume, log	
	Coefficient	***P* Value**	**Coefficient**	***P* Value**	**Coefficient**	***P* Value**
Foveal layers						
Total RT						
HIV-infected	0.393	0.361	−0.260	0.471	0.003	0.827
Healthy	1.020	0.011*	0.649	0.052	−0.007	0.485
GCL						
HIV-infected	−0.827	0.738	0.398	0.846	−0.005	0.934
Healthy	4.561	0.005*	3.408	0.011*	−0.010	0.818
IPL						
HIV-infected	0.221	0.920	−1.461	0.423	−0.023	0.674
Healthy	2.936	0.106	1.507	0.311	−0.001	0.985
INL						
HIV-infected	1.029	0.656	−1.833	0.331	−0.051	0.384
Healthy	3.950	0.048*	3.053	0.060	−0.014	0.784
ONL+IS						
HIV-infected	0.915	0.192	−0.307	0.609	0.026	0.170
Healthy	1.859	0.024*	0.612	0.378	−0.020	0.326
Pericentral layers						
Total RT						
HIV-infected	0.557	0.257	0.064	0.879	0.002	0.856
Healthy	1.286	0.015*	0.443	0.318	−0.016	0.257
GCL						
HIV-infected	0.174	0.916	1.240	0.369	−0.042	0.304
Healthy	3.620	0.023*	1.857	0.157	−0.030	0.492
IPL						
HIV-infected	0.373	0.881	1.113	0.591	−0.091	0.149
Healthy	3.370	0.200	0.600	0.781	−0.077	0.248
INL						
HIV-infected	3.160	0.176	−0.680	0.728	−0.050	0.403
Healthy	4.394	0.108	1.911	0.403	−0.051	0.467
ONL+IS						
HIV-infected	0.982	0.295	−0.005	0.995	0.046	0.051
Healthy	1.819	0.050*	0.533	0.492	−0.006	0.799

Results of the pooled regression analysis evaluating the relationship between retinal layer thickness and cerebral volume. The regression model included retinal layer thickness, which was stratified between HIV-infected children and controls (as displayed in the table), and covariables HIV status, age, sex, SE, and ICV (not shown). Coefficients represent changes in volume (cm^3) per micron increase in RT. INL, inner nuclear layer.

* $P < 0.05$.

diffusivity changes, yet to a lesser degree, that does not lead to a detectable group difference.

Significant associations between RT and cerebral volume (in particular GM volume) were detected in healthy children only, implying a physiological relationship between RT and GM volume. This seems plausible, since both retina and GM largely consist of unmyelinated neuronal cells.[7] A previous study also described a correlation between GM volume and inner retinal layer thickness (GC–IPL) in healthy participants without glaucoma or clinical retinal disease, although this was a study assessing neurodegeneration in elderly individuals (with patients over 60 years of age),[18] limiting comparability to our

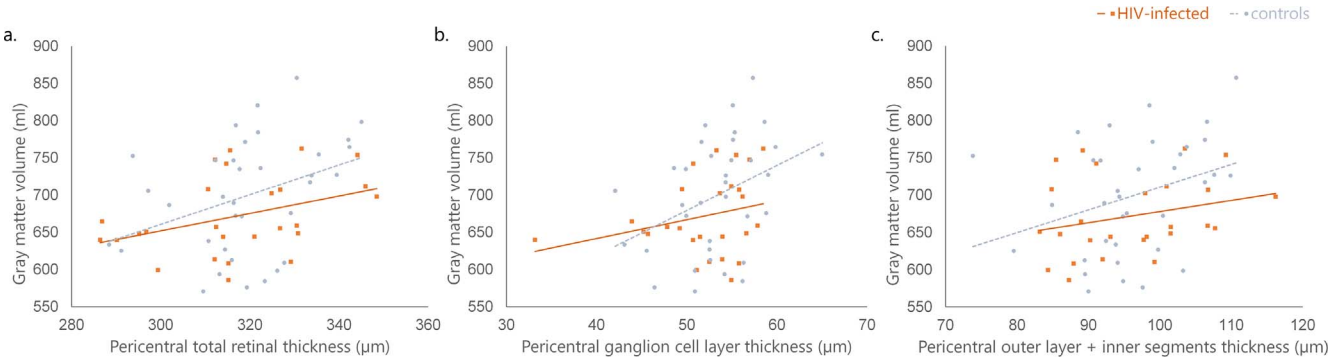

Figure 2. Univariable scatter and linear fit plots illustrating the relationships between GM volume and pericentral total retinal thickness (**a**), pericentral ganglion cell layer thickness (**b**) and pericentral outer layer + inner segments thickness (**c**) in healthy controls (*dashed lines*). These associations were less pronounced, and not statistically significant, in HIV-infected children (*solid lines*).

pediatric study population. Nonetheless, currently there are no other studies comparing MRI and OCT in healthy individuals or children.

In HIV-infected children, the relationship between RT and cerebral volume for the most part paralleled that of healthy children, but without reaching statistical significance, even though both RT[6] and cerebral volume[4] were significantly reduced in the HIV-infected children of our cohort. This might indicate that a physiological relationship between RT and cerebral volume—as detected in healthy children—is disturbed in HIV-infected children. However, a difference between HIV-infected children and controls in the association between RT and cerebral volume was only detected for a single retinal layer (as shown in Supplementary Table S4), which may partly be caused by lack of statistical power for the associations for the other retinal layers due to the relatively low number of subjects.

The absence of an association between RT and cerebral volume in HIV-infected children contrasts with the presence of multiple associations between RT and WM diffusivity in HIV-infected children. This may suggest a difference in the pathogenesis of the microstructural retinal and WM changes on the one hand, and of macrostructural cerebral volume changes on the other hand. Firstly, this distinction could reflect different timing of the impact of HIV infection on retinal and cerebral structures, i.e., progressive ongoing injury versus stable injury or delayed maturation as residual effects of (unsuppressed) HIV infection early in life. Previously detected associations of cerebral and retinal impairments with historical HIV disease markers, such as lower nadir $CD4^+$ T-cell count, higher peak HIV viral load, and an acquired immunodeficiency syndrome (AIDS) diagnosis, provide substantial support for the relevance of lingering HIV-induced damage in the pathogenesis of all observed changes.[4,6] However, the course of retinal and neurostructural abnormalities over time in the context of potent cART can only be evaluated in a longitudinal setting. There may also be different contributions of underlying HIV-related pathogenic mechanisms, e.g., direct HIV neurotoxicity, chronic HIV-induced neuroinflammation, vascular dysfunction, cerebral perfusion changes, or (long-term) cART toxicity, that can exert different effects on the various cells and systems within the brain, resulting in different types of injury.[2]

Unmeasured factors unrelated to the HIV-infection itself might also have been at play, such as detrimental early life circumstances that may have hindered normal brain development.[19–21] Indeed, early life malnutrition has been linked to cortical atrophy,[20] which may have occurred more frequently among HIV-infected participants, due to a larger proportion of immigrants in that group. Furthermore, we did not have reliable information regarding prematurity of these children, which might have affected both retinal and cerebral development.[22,23]

Despite being the largest and first combined OCT/MRI study in cART-treated HIV-infected children without retinitis to date, using a highly similar control group, this study is subject to several limitations. First, the modest sample size may have limited our power to detect potentially clinically relevant associations. Second, as this was an exploratory study, we did not adjust for multiple comparisons. Nonetheless, we detected a substantial number of significant associations, and the overall pattern and direction of the observed associations between RT and WM diffusivity in HIV-infected children, and RT and GM volume in healthy children, were consistent with our predictions and pathophysiological models, making it unlikely that our findings were spurious. Third, a detailed assessment of specific brain areas might reveal stronger associations with RT than the global MRI measures we currently used. Finally, this cross-sectional study does not explain the mechanisms underlying the associations observed between retinal and cerebral changes.

To conclude, in this cross-sectional study we observed that RT is correlated with WM microstructural alterations, but not with cerebral volume in perinatally HIV-infected children on cART. These findings support OCT as a noninvasive, rapid, and relatively inexpensive adjuvant tool to assess WM changes in this population, and provide a rationale for conducting longitudinal studies assessing retinal and cerebral changes and relations over time. To explore how different HIV-related pathogenic mechanisms contribute to retinal structural abnormalities and different types of cerebral injury, future studies should assess the relationship of these OCT and MRI outcomes with markers of inflammation, immune activation, vascular endothelial function, and neurodegeneration in cerebrospinal fluid and blood. Furthermore, comparing retinal and cerebral abnormalities between perinatally HIV-infected children and individuals who acquired HIV as adults may further contribute to our understanding of the role of brain maturation, early life exposure to HIV, and lifelong cART in the pathogenesis of pediatric HIV-induced retinal and cerebral injury.

Acknowledgments

Data were in part presented previously at the 15th European AIDS Conference on October 21–24, 2015, in Barcelona, Spain and at The Netherlands Conference on HIV Pathogenesis, Epidemiology, Prevention and Treatment (NCHIV) on November 18, 2015, in Amsterdam, The Netherlands, and included in the respective conference abstract books.

Supported by Bayer Healthcare's Global Ophthalmology Awards Program 2012 and the Emma Foundation (Grant 11.001). These funding bodies had no role in the design or conduct of the study, nor in the analysis or interpretation of the results. MA's institution received research grants (NIH, NSF, JDRF). PR's institution has received research grants (Gilead Sciences, ViiV Healthcare, Janssen Pharmaceutica, Bristol Myers Squibb, and Merck). DP's institution has received research grants from Emma Foundation, AIDS Fonds, and ViiV Healthcare.

Disclosure: **C. Blokhuis**, None; **N. Demirkaya**, None; **S. Cohen**, None; **F.W.N.M. Wit**, None; **H.J. Scherpbier**, None; **P. Reiss**, None; **M.D. Abramoff**, IDxLLC (C, S), University of Iowa (F, R) P; **M.W.A. Caan**, None; **C.B.L.M. Majoie**, None; **F.D. Verbraak**, Bayer (C, R), Novartis (C); **D. Pajkrt**, None

References

1. Patel K, Ming X, Williams PL, Robertson KR, Oleske JM, Seage GR. Impact of HAART and CNS-penetrating antiretroviral regimens on HIV encephalopathy among perinatally infected children and adolescents. *AIDS*. 2009;23:1893–1901.
2. Blokhuis C, Kootstra NA, Caan MW, Pajkrt D. Neurodevelopmental delay in pediatric HIV/AIDS: current perspectives. *Neurobehav HIV Med*. 2016;7:1–13.
3. Hoare J, Ransford GL, Phillips N, Amos T, Donald K, Stein DJ. Systematic review of neuroimaging studies in vertically transmitted HIV positive children and adolescents. *Metab Brain Dis*. 2014;29:221–229.
4. Cohen S, Caan MWA, Mutsaerts HJ, et al. Cerebral injury in perinatally HIV-infected children compared to matched healthy controls. *Neurology*. 2016;86:19–27.
5. Cohen S, Stege JA, Geurtsen GJ, et al. Poorer cognitive performance in perinatally HIV-infected children versus healthy socioeconomically matched controls. *Clin Infect Dis*. 2015;60:1111–1119.
6. Demirkaya N, Cohen S, Wit FWNM, et al. Retinal structure and function in perinatally HIV-infected and cART-treated children:

a matched case-control study. *Invest Ophthalmol Vis Sci*. 2015;56:3945–3954.

7. London A, Benhar I, Schwartz M. The retina as a window to the brain-from eye research to CNS disorders. *Nat Rev Neurol*. 2013;9:44–53.
8. Balk LJ, Petzold A. Current and future potential of retinal optical coherence tomography in multiple sclerosis with and without optic neuritis. *Neurodegener Dis Manag*. 2014;4: 165–176.
9. Ikram MK, Cheung CY, Wong TY, Chen CPLH. Retinal pathology as biomarker for cognitive impairment and Alzheimer's disease. *J Neurol Neurosurg Psychiatry*. 2012; 83:917–922.
10. Sari ES, Koc R, Yazici A, Sahin G, Ermis SS. Ganglion cell-inner plexiform layer thickness in patients with Parkinson disease and association with disease severity and duration. *J Neuroophthalmol*. 2015;35:117–121.
11. Schönfeldt-Lecuona C, Kregel T, Schmidt A, et al. From imaging the brain to imaging the retina: optical coherence tomography (OCT) in schizophrenia. *Schizophr Bull*. 2016;42: 9–14.
12. Garvin MK, Abramoff MD, Kardon R, Russell SR, Wu X, Sonka M. Intraretinal layer segmentation of macular optical coherence tomography images using optimal 3-D graph search. *IEEE Trans Med Imaging*. 2008;27:1495–1505.
13. Garvin MK, Abràmoff MD, Wu X, Russell SR, Burns TL, Sonka M. Automated 3-D intraretinal layer segmentation of macular spectral-domain optical coherence tomography images. *IEEE Trans Med Imaging*. 2009;28:1436–1447.
14. Demirkaya N, van Dijk HW, van Schuppen SM, et al. Effect of age on individual retinal layer thickness in normal eyes as measured with spectral-domain optical coherence tomography. *Invest Ophthalmol Vis Sci*. 2013;54:4934–4940.
15. van Dijk HW, Verbraak FD, Kok PHB, et al. Decreased retinal ganglion cell layer thickness in patients with type 1 diabetes. *Invest Ophthalmol Vis Sci*. 2010;51:3660–3665.
16. Gordon-Lipkin E, Chodkowski B, Reich DS, et al. Retinal nerve fiber layer is associated with brain atrophy in multiple sclerosis. *Neurology*. 2007;69:1603–1609.
17. Grazioli E, Zivadinov R, Weinstock-Guttman B, et al. Retinal nerve fiber layer thickness is associated with brain MRI outcomes in multiple sclerosis. *J Neurol Sci*. 2008;268:12–17.
18. Ong Y-T, Hilal S, Cheung CY, et al. Retinal neurodegeneration on optical coherence tomography and cerebral atrophy. *Neurosci Lett*. 2015;584:12–16.
19. Behnke M, Smith VC. Prenatal substance abuse: short- and long-term effects on the exposed fetus. *Pediatrics*. 2013;131: e1009–e1024.
20. Potchen MJ, Kampondeni SD, Mallewa M, Taylor TE, Birbeck GL. Brain imaging in normal kids: a community-based MRI study in Malawian children. *Trop Med Int Health*. 2013;18: 398–402.
21. van Harmelen AL, van Tol M, van der Wee NJA, et al. Reduced medial prefrontal cortex volume in adults reporting childhood emotional maltreatment. *Biol Psychiatry*. 2010;68:832–838.
22. Nosarti C, Nam KW, Walshe M, et al. Preterm birth and structural brain alterations in early adulthood. *NeuroImage Clin*. 2014;6:180–191.
23. Vajzovic L, Rothman AL, Tran-Viet D, Cabrera MT, Freedman SF, Toth CA. Delay in retinal photoreceptor development in very preterm compared to term infants. *Invest Ophthalmol Vis Sci*. 2015;56:908–913.

Investigative Ophthalmology & Visual Science